# Classification of higher order diagrams in non-equilibrium theory, and the removal of pinch singularities

D. S. Isert* and S. P. Klevansky†
*Institut für Theoretische Physik,*
*Philosophenweg 19, D-69120 Heidelberg, Germany*



## Abstract

The non-equilibrium two loop self-energy is reexamined in the framework of a scalar quark and gluon model, with specific attention to terms which do not give rise to the standard two → two particle collisional terms in the semi-classical Boltzmann equation. It is shown that most of these terms contribute to renormalization of component lines at a lower level, rendering the theory correct to $g^4m^4$. This result can be generalized to a higher number of loops. The remaining terms, which do not fall into any physical category, are shown explicitly to vanish. We then examine the possibility that pinch singularities could arise in this theory, and demonstrate that this is not so for the case of equilibrium and small deviations from equilibrium, at the two loop level.

PACS Numbers : 05.20.Dd; 11.10.Wx; 24.85.+p; 12.38.Mh
Keywords: Transport theory; pinch singularities; non-equilibrium quantum field theory

*E-mail: D.Isert@tphys.uni-heidelberg.de

†Current address: DB AG, Kleyerstr.27, D-60236 Frankfurt a. M., Germany

## I. INTRODUCTION

Due to the short time span of a heavy-ion collision, it is believed that a non-equilibrium description of such a collision may be necessary to give a complete and adequate description of the particle evolution. Several reviews of the non-equilibrium approach in general may be found in [1]. For heavy ion collisions, heuristic models have been developed, which are guided by the approach of Boltzmann, that presumes that only two body collisions can occur. These can then be generalized in an heuristic fashion [2]. On the other hand, from the field theoretical point of view, there have been many attempts to generate the correct and appropriate non-equilibrium theory for a given Lagrangian (see, for example [3]. Often these stop at the mean-field level, due to the inherent complexity of the non-equilibrium formalism per se. In some previous works, the two-body collisional term has been calculated for a static potential interaction, and under many simplifying assumptions in [4]. Although a graphical series was given for the two loop self-energy following from a Walecka type interaction in [5], the physical interpretation of all the terms that occur in this series or direct expressions for them was not given. Note that the difficulty lies in the fact that the non-equilibrium formalism generates far more diagrams of a given topology than does the equilibrium zero temperature or Matsubara finite temperature formalism which generates Feynman graphs in the standard way. In a broad sense, the ultimate goal which we have, is to obtain a complete physical understanding of *all* the additional terms (over and above those which are expected from a Feynman diagram point of view) that are generated in the non-equilibrium formalism, in order that a precise formulation in, for example, the study of non-equilibrium evolution of distribution functions in QCD, rather than simply a heuristic approach, can be made. At this stage, however, we restrict ourselves to far simpler systems.

In this paper, we examine the collisional integral for a scalar quark-gluon model in the Hartree-Fock approximation and for the two loop diagrams in greater detail than before [6], placing specific emphasis on the extra terms that are naturally generated in the non-equilibrium formalism. In this study, (a) we are able to show that two-loop diagrams that were previously ignored [6] as they do not contribute directly to the two-particle scattering terms expected from classical Boltzmann theory, do in fact have an important physical relevance: all of these remaining graphs

are required to correct the *lower* order tree level graphs which give rise to absorption or radiation processes and which also occur as matrix elements in the Boltzmann equation to one loop, implying that a simulation of a non-equilibrium process with this or similar models requires inclusion of such terms. (b) Our study is carried out within the Schwinger-Keldysh formalism [7] for non-equilibrium processes. Within this (and other) formulations of real-time finite temperature processes [8], the issue of pinch singularities arises (see for example [9–11]). This addresses the question as to whether the theory is well-defined or not, in that it possesses divergences that arise apparently from integration along the real axis of products of retarded and advanced Green functions $G_R G_A$. Such products occur naturally in the so-called 'retarded-advanced' (RA) version of the non-equilibrium formalism, which is an alternative way of presenting the Schwinger-Keldysh Green functions [12]. Alternately, pinch singularities manifest themselves as products of delta functions within the standard representation which we follow here. Within our model, we investigate the occurrence of pinch singularities in the series for the self-energy up to two loops and come to the conclusion that no pinch singularities occur.

To be specific, we utilize the scalar partonic model [13,14], defined by the Lagrangian

$$\begin{aligned}\mathcal{L} = {} & \partial^\mu \phi^{\dagger i,l} \partial_\mu \phi_{i,l} + \frac{1}{2}\partial^\mu \chi_{a,r} \partial_\mu \chi^{a,r} - \frac{m^2}{2}\chi_{a,r}\chi^{a,r} \\ & - gm\phi^{\dagger i,l}(T^a)^j_i (T^r)^m_l \phi_{j,m}\chi_{a,r} - \frac{gm}{3!} f_{abc} f_{rst} \chi^{a,r}\chi^{b,s}\chi^{c,t} \end{aligned} \tag{1.1}$$

in which scalar quark fields $\phi^{i,l}$ are coupled to scalar gluonic fields $\chi^{a,r}$ via a cubic interaction. The color indices $i, l = 1..N_c$, while $a, r = 1..(N_c - 1)$, reflects the product groups $SU(N_c) \times SU(N_c)$.

## II. COLLISION TERM TO TWO LOOPS

In order to recover the semi-classical extension of the Boltzmann equation, it is necessary to evaluate constructs of the form [4,6]

$$\begin{aligned} I_{\rm coll} &= \Pi^{-+}(X,p) D^{+-}(X,p) - \Pi^{+-}(X,p) D^{-+}(X,p) \\ &= I^{\rm gain}_{\rm coll} - I^{\rm loss}_{\rm coll}, \end{aligned} \tag{2.1}$$

where $D^{ij}(X,p)$, $i = +, -$ are Green functions of the standard Schwinger-Keldysh kind, and which are given in Appendix A. The transport and constraint equations

are briefly summarized in this Appendix also. The $\Pi^{ij}$ are the Wigner transformed self-energies of the associated particle. To be specific, we consider for the moment the self-energies and Green functions pertaining to the quark sector, $\Pi^{ij}(X,p) = \Sigma^{ij}(X,p)$ and $D^{ij}(X,p) = S^{ij}(X,p)$. The analysis for the gluonic sector follows then simply by inspection. Let us consider first the loss term. This means we need to calculate $\Sigma^{+-}(X,p)$. The quark self-energy to one loop is shown in Fig.1a) which is the Fock term, and to two loops in Fig.2. As there are many graphs at the two loop level, we make a structural classification of these according to their topology. We identify rainbow graphs (R), ladder graphs (L), cloud graphs (C), exchange graphs (E) and quark-loop graphs (QL). In [6], we were able to show explicitly that the Fock term of Fig.1a) leads to the requirement that the process $q\bar{q} \to g$, as given by Fig.1b), be incorporated into the associated Boltzmann equation at this level. We have also shown that the seven diagrams R a), L a), C a), C b), E a), E b) and QL a) are all essential for constructing the direct cross-sections of the processes $qq \to qq$, $q\bar{q} \to q\bar{q}$, $q\bar{q} \to gg$, and $qg \to qg$ which are shown in Fig3, and which then appear in the newly calculated Boltzmann equation that should be correct to the two loop level. Two questions now arise naturally. Firstly, one may ask what the purpose of the remaining thirteen graphs is, and secondly, more subtly, would they harbour divergences such as arise through pinch singularities, thereby rendering the theory ill-defined. In a previous paper, the remaining thirteen two-loop self-energy diagrams shown in Fig.2 were argued heuristically to be 'non-leading', and graphs of this type have up to now simply been ignored. Here, we wish to demonstrate precisely that these graphs in fact either vanish or contribute to corrections of order $g^3m^3$ to the lower order process $q\bar{q} \to g$. To demonstrate this, we arbitrarily examine the set of quark-loop diagrams. The QL a) graph of Fig.2 leads directly to the $qq$ and $q\bar{q}$ cross sections of Fig.3. On the other hand, the three graphs, QL b)-d) of Fig.2 which were *not* required for the evaluation of the cross-sections as derived for Fig.3. Let us examine each of these terms in turn. We commence with the diagram QL b) of Fig.2 which is given by

$$\begin{aligned}\Sigma^{(2)+-}_{\mathrm{q-Loop,b)}}(X,p) = -g^4m^4F^2_{\mathrm{q-Loop}}\int \frac{d^4p_1}{(2\pi)^4}\frac{d^4p_2}{(2\pi)^4}\frac{d^4p_3}{(2\pi)^4}\frac{d^4p_4}{(2\pi)^4}(2\pi)^4\delta^{(4)}(p-p_1-p_2)\\ \times(2\pi)^4\delta^{(4)}(p_2-p_3+p_4)\,S^{+-}(X,p_1)\,G^{+-}(X,p_2)\\ \times G^{++}(X,p_2)\,S^{++}(X,p_3)\,S^{++}(X,p_4),\end{aligned} \tag{2.2}$$

where $F^2_{\rm q-Loop}$ is the color factor for the two color $SU(N_c)$ groups. The corresponding loss term of the collision integral to this self-energy is defined by

$$J^{(2)\rm loss}_{\rm coll,q-Loop,b)} = -i\frac{\pi}{E_p}\Sigma^{(2)+-}_{\rm q-Loop,b)}(X, p^0 = E_p, \vec{p}) f_q(X, \vec{p}). \tag{2.3}$$

In this expression, the product $iS^{+-}(X, p_1)iG^{+-}(X, p_2)f_q(X, \vec{p})$ occurs. Inserting the quasiparticle approximation for the Green functions that are given in appendix A, we obtain for this product the sum of four terms:

$$\begin{aligned}
T_1 &= \frac{\pi}{E_1}\frac{\pi}{E_2}\delta(E_1 - p_1^0)\delta(E_2 - p_2^0)\bar{f}_q(X, p_1)\bar{f}_g(X, p_2)f_q(X, \vec{p}) \\
T_2 &= \frac{\pi}{E_1}\frac{\pi}{E_2}\delta(E_1 - p_1^0)\delta(E_2 + p_2^0)\bar{f}_q(X, p_1)f_g(X, -p_2)f_q(X, \vec{p}) \\
T_3 &= \frac{\pi}{E_1}\frac{\pi}{E_2}\delta(E_1 + p_1^0)\delta(E_2 - p_2^0)f_{\bar{q}}(X, -p_1)\bar{f}_g(X, p_2)f_q(X, \vec{p}) \\
T_4 &= \frac{\pi}{E_1}\frac{\pi}{E_2}\delta(E_1 + p_1^0)\delta(E_2 + p_2^0)f_{\bar{q}}(X, -p_1)f_g(X, -p_2)f_q(X, \vec{p}).
\end{aligned} \tag{2.4}$$

By attributing $f$ to incoming particles and $\bar{f}$ to outgoing ones, we see that $T_1 ... T_4$ correspond to the processes $q \to qg$, $qg \to q$, $q\bar{q} \to g$ and $q\bar{q}g \to \emptyset$. Since the quarks are massless while the gluons are endowed with a finite mass, the processes corresponding to $T_1$, $T_2$ and $T_4$ are kinematically forbidden as also occurred in the discussion of the Fock term in [6]. One thus has one remaining non-vanishing contribution $iS^{+-}(X, p_1)iG^{+-}(X, p_2)f_q(X, \vec{p}) = T_3$. This product is now inserted into Eq.(2.3). In the resulting expression, we interchange $p_1$ with $-p_1$ and on performing the $p_1^0$, $p_2^0$ and $p_4$ integrations, we find the result

$$\begin{aligned}
J^{(2)\rm loss}_{\rm coll,q-Loop,b)} = -i\frac{\pi}{E_p}g^4 m^4 F^2_{\rm q-Loop}\int \frac{d^3p_1}{(2\pi)^3 2E_1}\frac{d^3p_2}{(2\pi)^3 2E_2}\frac{d^4p_3}{(2\pi)^4}(2\pi)^4\delta^{(4)}(p + p_1 - p_2) \\
\times G^{++}(X, p_2)\, S^{++}(X, p_3)\, S^{++}(X, p_3 - p_2) f_{\bar{q}}(X, \vec{p}_1)\bar{f}_g(X, \vec{p}_2) f_q(X, \vec{p})
\end{aligned} \tag{2.5}$$

as the remaining contribution of the QL b) graph to the collision integral.

Now, in Fig.4, we independently examine the Feynman diagrams for the process $q\bar{q} \to g$ up to order $g^3 m^3$. The scattering amplitude associated with Fig.4a) has purely a point-like structure with color groups occurring:

$$-i\mathcal{M}^{a)}_{q\bar{q}\to g} = -igmt^a_{ij} \otimes t^r_{lm} \tag{2.6}$$

while from Fig.4b), one has

$$-i\mathcal{M}^{b)}_{q\bar{q}\to g} = g^3 m^3 [t^b_{ji}\mathrm{tr}(t^b t^a)] \otimes [t^s_{ml}\mathrm{tr}(t^s t^r)] G^{--}(X, p_2) \times \int \frac{d^4p_3}{(2\pi)^4} S^{--}(X, p_3)\, S^{--}(X, p_3 - p_2), \tag{2.7}$$

where $t^a_{ij}$ is the matrix of the color group in the representation of the quarks. Now note that using the fact that $[iG^{--}]^\dagger = iG^{++}$ and $F_{\mathrm{q-Loop}} = t^a_{ij} t^b_{ji} \mathrm{tr}(t^b t^a)$, one can rewrite Eq.(2.5) in terms of these matrix elements, i.e.

$$J^{(2)\mathrm{loss}}_{\mathrm{coll,q-Loop,b)}} = \frac{\pi}{E_p} \int \frac{d^3p_1}{(2\pi)^3 2E_1} \frac{d^3p_2}{(2\pi)^3 2E_2} (2\pi)^4 \delta^{(4)}(p + p_1 - p_2) \times \mathcal{M}^{a)}_{q\bar{q}\to g} [\mathcal{M}^{b)}_{q\bar{q}\to g}]^\dagger f_q(X, \vec{p}) f_{\bar{q}}(X, \vec{p}_1) \bar{f}_g(X, \vec{p}_2), \tag{2.8}$$

illustrating that the cross term between these two processes, denoted symbolically as $a^\dagger b$, is derived from the self-energy diagram QL b) of Fig.2. The gain term can be obtained by replacing $f$ with $\bar{f}$ and vice versa in Eq.(2.8).

In a similar fashion, the collision integral can be constructed from the quark-loop diagram QL c) in Fig.2. One obtains an expression for the loss term as in Eq.(2.5) with $iG^{++}iS^{++}iS^{++}$ replaced by the combination $iG^{--}iS^{--}iS^{--}$. Again $J^{(2)\mathrm{loss}}_{\mathrm{coll,q-Loop,b)}}$ can be expressed by the scattering amplitudes of Eq.(2.6) and (2.7):

$$J^{(2)\mathrm{loss}}_{\mathrm{coll,q-Loop,c)}} = \frac{\pi}{E_p} \int \frac{d^3p_1}{(2\pi)^3 2E_1} \frac{d^3p_2}{(2\pi)^3 2E_2} (2\pi)^4 \delta^{(4)}(p + p_1 - p_2) \times [\mathcal{M}^{a)}_{q\bar{q}\to g}]^\dagger \mathcal{M}^{b)}_{q\bar{q}\to g} f_q(X, \vec{p}) f_{\bar{q}}(X, \vec{p}_1) \bar{f}_g(X, \vec{p}_2), \tag{2.9}$$

i.e. the second cross term $b^\dagger a$ required in building a cross-section of the basic component a) and b) of Fig.4 is required.

In an analogous fashion, one can show that the rainbow diagrams R b) and c) lead to a collision integral containing $\mathcal{M}^{a)}_{q\bar{q}\to g}[\mathcal{M}^{f)}_{q\bar{q}\to g}]^\dagger$ and the hermitian conjugate of this product, the ladder diagrams Lb) and c) to a collision integral containing $\mathcal{M}^{a)}_{q\bar{q}\to g}[\mathcal{M}^{c)}_{q\bar{q}\to g}]^\dagger$ and its hermitian conjugate, the cloud diagrams C c) and d) to a collision integral containing $\mathcal{M}^{a)}_{q\bar{q}\to g}[\mathcal{M}^{d)}_{q\bar{q}\to g}]^\dagger$ and its hermitian conjugate, and finally the exchange diagrams E c) and d) to a collision integral containing $\mathcal{M}^{a)}_{q\bar{q}\to g}[\mathcal{M}^{e)}_{q\bar{q}\to g}]^\dagger$ and its hermitian conjugate. Note that in this fashion, we are able to account for all mixed diagrams that would occur in the construction of the $|\mathcal{M}_{q\bar{q}\to g}|^2$ up to order $g^4m^4$, with the exception of the diagram g) of Fig.4. This graph does not enter into the collision integral, as it is a renormalization diagram for the *incoming* quark, for which the momentum $p$ is fixed externally.

Returning to our explicit example of the quark-loop self-energy of Fig.2, one sees that a simple graphical interpretation can be applied to each figure. A rule in which all lines that are connected by $\pm$ and $\mp$ are cut in a single path, separates the graphs QL a)-c) into their component matrix elements. This is illustrated in Fig.5. This procedure, however, cannot be applied uniquely to the graph QL d), nor for that matter to the remaining graphs which are not required for construction of the mixed terms or direct contributions to the cross-sections, i.e. the graphs R d) and L d). We are thus now left with the three graphs QL d), R d) and L d) which at first sight fit into no apparent scheme, and which therefore may present difficulties.

We commence with the investigation of QL d). For this self-energy we obtain an expression as in Eq.(2.2) with the product of the five Green functions replaced by $S^{+-}(X,p_1)[G^{+-}(X,p_2)]^2S^{-+}(X,p_3)S^{+-}(X,p_4)$. In the quasi-particle approximation the off-diagonal Green functions are on mass shell:

$$p_1^2 = p_3^2 = p_4^2 = 0 \tag{2.10}$$

$$p_2^2 = m^2 \tag{2.11}$$

In addition to this, the two $\delta$-functions for the energy-momentum conservation of Eq.(2.2) have to be fullfilled. Therefore we can write for example

$$0 = p_3^2 = (p_2 + p_4)^2 = 2p_2p_4 + m^2. \tag{2.12}$$

Together with Eq.(2.11) this leads to

$$p_4 = -\frac{1}{2}p_2 \quad => \quad p_4^2 = \frac{1}{4}p_2^2 = \frac{1}{4}m^2 > 0. \tag{2.13}$$

This is inconsistent with Eq.(2.10) and therefore $\Sigma^{(2)+-}_{\mathrm{q-Loop,d)}}$ has to vanish. A similar investigation of the graphs R d) and L d) shows that they vanish for the same reason.

So far we have derived the results for two loop self-energy diagrams in detail. Let us summarize now the results for self-energy diagrams with more than two loops. The result obtained in this section can be generalized easily to three and more loops. Including the three loop self-energy into the collision term leads to cross sections of all possible processes with two (three) partons in the initial state and three (two) partons in the final state. Furthermore, they give all additional corrections of order $g^6m^6$ to the process $q\bar{q} \to g$, e.g. the product of scattering amplitudes of the diagrams b)-f) in Fig.4, and also corrections to all scattering processes of two partons into two partons, $qq \to qq$, $q\bar{q} \to q\bar{q}$, $q\bar{q} \to gg$ and $qg \to qg$.

## III. PINCH SINGULARITIES

To investigate the issue of pinch singularities, let us make two simplifing assumptions: a) the self-energies are calculated at zero momentum and b) we do not distinguish between quarks and gluons. The latter assumption reduces the number of generic two loop self-energy diagrams from five to two, shown in Fig.6. The first type, the rainbow diagram, is shown for $\Sigma_R^{--}$ and $\Sigma_R^{-+}$ in more detail in Fig.7. From these two self-energies, the retarded self-energy can be constructed as

$$\Sigma_R^r = \Sigma_R^{--} + \Sigma_R^{-+}. \tag{3.1}$$

Since the retarded self-energy is a physically relevant property, that enters, for example, into the constraint equation Eq.(A5), we want to investigate the diagrams of Fig.7 in more detail. In each of the diagrams b), c) and f) of Fig.7, it is possible to identify an internal vertex to which lines three off-diagonal Green functions are attached. Since these Green functions are on mass shell, this corresponds to a decay of an on-shell particle into two on-shell particles of the same species. This is a forbidden process, and therefore these three diagrams vanish. Closer inspection of Fig.7 g) shows that the momentum structure of the Green functions is similar to that of b), c) and f), and this graph is therefore also vanishing. Consequently, $\Sigma_R^r$ is the sum of the remaining diagrams a), d), e) and h):

$$\begin{aligned}\Sigma_R^r(X,0) = (-igm)^4 \int \frac{d^4k}{(2\pi)^4}\frac{d^4l}{(2\pi)^4} \Big\{ & [D^{--}(k)]^3 D^{--}(k-l) D^{--}(l) \\ & + D^{--}(k)[D^{-+}(k)]^2 D^{++}(k-l) D^{++}(l) \\ & - D^{--}(k)[D^{-+}(k)]^2 D^{--}(k-l) D^{--}(l) \\ & - D^{++}(k)[D^{-+}(k)]^2 D^{++}(k-l) D^{++}(l) \Big\}. \end{aligned} \tag{3.2}$$

This construction appears to contain pinch singularities, evidenced by the fact that products of $D(k)$ occur, and it is imperative to show that the apparent divergence vanishes through cancellation. For simplicity, we consider this problem first in equilibrium. We do this for two reasons. Firstly, a correct calculation in equilibrium should be entirely free of pinch singularities, as has been demonstrated generally in [15]. In addition, calculations can be simplified dramatically, in such a fashion as to allow for an extension to systems slightly off equilibrium in a simple fashion in

this direct example. We use the following reasoning: in equilibrium, the Schwinger-Keldysh contour is simply one of a family of choices of contour in which the upper and lower integration routes are separated by a distance $\sigma$, and with which a form of real time field theory [RTFT] is generated [16]. In the Schwinger-Keldysh case, one makes the choice $\sigma = 0$. Physical quantites, when calculated, should however be independent of the value of $\sigma$. As it turns out, the particular value $\sigma = 1/2$, which generates the so-called thermo field theory (TFT) formalism [17], gives distinct calculational advantages, as products of off-diagonal elements can be seen to simply vanish. Given this equivalence, we are free to choose to do our analysis in the TFT framework.

The scalar Green functions, in the TFT formalism, are given as

$$\begin{aligned}\begin{pmatrix} iD^{--} & iD^{-+} \\ iD^{+-} & iD^{++} \end{pmatrix} &= \begin{pmatrix} D_0^1 + D_\beta & D'_\beta \\ D'_\beta & D_0^2 + D_\beta \end{pmatrix} \\ &= \begin{pmatrix} \frac{i}{k^2-m^2+i\epsilon} + \frac{2\pi\delta(k^2-m^2)}{e^{\beta|k_0|}-1} & 2\pi\delta(k^2-m^2)\frac{e^{\beta|k_0|/2}}{e^{\beta|k_0|}-1} \\ 2\pi\delta(k^2-m^2)\frac{e^{\beta|k_0|/2}}{e^{\beta|k_0|}-1} & \frac{-i}{k^2-m^2-i\epsilon} + \frac{2\pi\delta(k^2-m^2)}{e^{\beta|k_0|}-1} \end{pmatrix}, \end{aligned} \tag{3.3}$$

so defining $D_0^1$, $D_0^2$, $D_\beta$ and $D'_\beta$[1]. Let us compare these Green functions with the ones in Eqs.(A10)- (A13). In equilibrium, $f_a(X,p) = f_a(X,-p) = 1/(e^{\beta|p_0|}-1)$. If we do not distinguish between particles and antiparticles, then the diagonal Green functions in the TFT formalism are equal to the ones in Eqs.(A12) and (A13). The off-diagonal Green functions differ from Eqs.(A10) and (A11). However, in the self-energies considered only the product $D^{-+}D^{+-}$ occurs, which is the same in both types of formalism. This in itself demonstrates that one may use the Green functions of the TFT formalism with impunity in the following discussion. We consider first the last term of the retarded self-energy in Eq.(3.2):

$$\begin{aligned}\int \frac{d^4l}{(2\pi)^4} D^{++}(k-l)D^{++}(l) &= \int \frac{d^4l}{(2\pi)^4} \Big\{ D_0^2(k-l)D_0^2(l) + D_0^2(k-l)D_\beta(l) \\ &\quad + D_\beta(k-l)D_0^2(l) + D_\beta(k-l)D_\beta(l) \Big\} \\ &= \int \frac{d^4l}{(2\pi)^4} \Big\{ -D_0^1(k-l)D_0^1(l) - D_0^1(k-l)D_\beta(l)\end{aligned}$$

[1]Our notation introduces a factor $i$ in the first matrix, in order to establish consistency with our Schwinger-Keldysh Green functions of Appendix A. This differs from the standard use of TFT users [18].

$$-D_\beta(k-l)D_0^1(l)+D_\beta(k-l)D_\beta(l)\Big\}$$
$$=-\int\frac{d^4l}{(2\pi)^4}D^{--}(k-l)D^{--}(l) \tag{3.4}$$

In the first step, we have made use of the relations [18]

$$\int\frac{d^4l}{(2\pi)^4}D_0^1(k-l)D_0^1(l)=-\int\frac{d^4l}{(2\pi)^4}D_0^2(k-l)D_0^2(l) \tag{3.5}$$

and

$$\int\frac{d^4l}{(2\pi)^4}D_0^1(k-l)D_\beta(l)=-\int\frac{d^4l}{(2\pi)^4}D_0^2(k-l)D_\beta(l). \tag{3.6}$$

In the second step, we have made use of the fact that the fourth term, $D_\beta(k-l)D_\beta(l)$, has to vanish, since together with $D'_\beta(k)$ of Eq.(3.2) it corresponds again to the decay of an on-shell particle into two on-shell particles. With Eq.(3.4), we can rewrite Eq.(3.2) for the retarded self-energy as

$$\Sigma_R^r(X,0)=(gm)^4\int\frac{d^4k}{(2\pi)^4}\frac{d^4l}{(2\pi)^4}D^{--}(k-l)D^{--}(l)$$
$$\times\left\{[D^{--}(k)]^3-2D^{--}(k)[D^{-+}(k)]^2+D^{++}(k)[D^{-+}(k)]^2\right\}. \tag{3.7}$$

It is now convenient to make use of the following representation of $\delta$-function,

$$2\pi\delta(k^2-m^2)=\frac{i}{k^2-m^2+i\epsilon}-\frac{i}{k^2-m^2-i\epsilon}$$
$$=D_0^1+D_0^2. \tag{3.8}$$

Then the term in curly brackets of Eq.(3.7) is evaluated to give

$$\{...\}=[D_0^1+(D_0^1+D_0^2)f_B]^3+[D_0^2+(D_0^1+D_0^2)f_B](D_0^1+D_0^2)^2g_B^2$$
$$-2[D_0^1+(D_0^1+D_0^2)f_B](D_0^1+D_0^2)^2g_B^2, \tag{3.9}$$

where $g_B=e^{\beta|k_0|/2}/(e^{\beta|k_0|}-1)$. Using the fact that $f_B^2-g_B^2=-f_B$, we find

$$\{...\}=(D_0^1)^3+[(D_0^1)^3+(D_0^2)^3]f_B. \tag{3.10}$$

This expression is well defined, since no products of $D_0^1D_0^2$ occur any longer. With the relation

$$(D_0^1)^3+(D_0^2)^3=-\frac{1}{2}\left(\frac{\partial}{\partial m^2}\right)^2(D_0^1+D_0^2)$$
$$=-\frac{1}{2}\left(\frac{\partial}{\partial m^2}\right)^2 2\pi\delta(k^2-m^2), \tag{3.11}$$

we can write the retarded self-energy as

$$\Sigma_R^r(X,0) = (gm)^4 \int \frac{d^4k}{(2\pi)^4}\frac{d^4l}{(2\pi)^4} D^{--}(k-l)D^{--}(l) \times \left\{ (D_0^1)^3 - \frac{1}{2}\left(\frac{\partial}{\partial m^2}\right)^2 2\pi\delta(k^2-m^2) f_B \right\}. \tag{3.12}$$

We conclude that for the retarded rainbow self-energy $\Sigma_R^r$ no pinch singularities occur.

We now have to consider the cloud self-energy of Fig.6(b). The retarded self-energy is constructed in a similar way as for the rainbow diagram. The calculation of such a diagram within the framework of $\phi^3$ theory has been performed in [18]. This result can be simply taken over for our purposes, and we quote the final expression here:

$$\Sigma_C^r(X,0) = (gm)^4 \int \frac{d^4k}{(2\pi)^4}\frac{d^4l}{(2\pi)^4} \left[\left(D_0^1(k)\right)^2 + \chi(k)\right] \times \left[D_0^1(k-l) + D_\beta(k-l)\right]\left[\left(D_0^1(l)\right)^2 + \chi(l)\right], \tag{3.13}$$

where the function

$$\begin{aligned} \chi(k) &= 2D_0^1 D_\beta + D_\beta^2 - (D'_\beta)^2 \\ &= 2P\frac{i}{k^2-m^2} 2\pi\delta(k^2-m^2) f_B \\ &= i\frac{\partial}{\partial m^2} 2\pi\delta(k^2-m^2) f_B \end{aligned} \tag{3.14}$$

is free of singularities. Thus we conclude that in equilibrium, the retarded self-energies with two loops have no pinch singularities. We conjecture that the inclusion of different kinds of particles interacting with each, as in Section II, will not display pinch singularities - the actual demonstration of this fact, however, is cumbersome.

Let us now investigate the effect of small deviations from equilibrium, i.e. we replace $f_B = 1/(e^{\beta|k_0|}-1)$ by $f_B + \delta f_B$ in Eq.(3.3). In deriving our result for the retarded self-energies $\Sigma_R^r$ and $\Sigma_C^r$, Eqs.(3.12) and (3.13), a central feature is that the relationship $f_B^2 - g_B^2 = -f_B$ was used. For small deviations from equilibrium, this becomes

$$\begin{aligned} f_B^2 &\to [f_B + \delta f_B]^2 \\ g_B^2 = f_B(1+f_B) &\to [f_B + \delta f_B][1 + f_B + \delta f_B] \end{aligned}$$

$$
\begin{aligned}
=> f_B^2 - g_B^2 \to [f_B + \delta f_B][f_B + \delta f_B - 1 - f_B - \delta f_B] \\
= -[f_B + \delta f_B], \qquad (3.15)
\end{aligned}
$$

i.e. it is still valid. Therefore we obtain for $\Sigma_R^r$ and $\Sigma_C^r$ expressions such as in Eqs.(3.12) and (3.13), respectively, with $f_B$ replaced by $f_B+\delta f_B$. Consequently, even for small deviations from equilibrium, no pinch singularities occur for the retarded self-energies up to two loops.

## IV. SUMMARY AND CONCLUSIONS

In this paper, we have demonstrated that for the two loop self-energy, the graphs which are generated in the non-equilibrium Schwinger-Keldysh formalism which do not contribute to two $\to$ two processes are either vanishing or are necessary to renormalize the graphs of one loop order to the same level of the coupling strength $g^4m^4$. This applies to all external legs, save the incoming leg, which is fixed externally. This result can be generalized to $n$ loops: self-energy graphs containing $n$-loops lead to contributions to the semiclassical Boltzmann equation that are $n \to n$ in nature plus include all permutations of the particles on the left and right hand sides [6]. In addition, however, graphs of lower order are renormalized successively to the same order of the coupling constant. We have illustrated that, to the two loop level, pinch singularities da not occur in the equilibrium formulation, as expected from Ref. [15] and by a simple extension of the technique here, for small deviations from equilibrium.

## V. ACKNOWLEDGMENTS

One of us (D.S.I.) thanks C. Greiner and S. Leupold for useful comments made during the course of this study.

## APPENDIX A: GREEN FUNCTIONS

In this Appendix, we list the Green functions used in Section II. In the Schwinger-Keldysh formalism [7] they are defined for the (scalar) quarks ($D = S$) as

$$
\begin{aligned}
iS^c(x,y) &= \left\langle T\phi^{i,l}(x)\phi^{\dagger j,m}(y)\right\rangle - \left\langle \phi^{i,l}(x)\right\rangle \left\langle \phi^{\dagger j,m}(y)\right\rangle = iS^{--}(x,y)\\
iS^a(x,y) &= \left\langle \tilde{T}\phi^{i,l}(x)\phi^{\dagger j,m}(y)\right\rangle - \left\langle \phi^{i,l}(x)\right\rangle \left\langle \phi^{\dagger j,m}(y)\right\rangle = iS^{++}(x,y)\\
iS^>(x,y) &= \left\langle \phi^{i,l}(x)\phi^{\dagger j,m}(y)\right\rangle - \left\langle \phi^{i,l}(x)\right\rangle \left\langle \phi^{\dagger j,m}(y)\right\rangle = iS^{+-}(x,y)\\
iS^<(x,y) &= \left\langle \phi^{\dagger j,m}(y)\phi^{i,l}(x)\right\rangle - \left\langle \phi^{i,l}(x)\right\rangle \left\langle \phi^{\dagger j,m}(y)\right\rangle = iS^{-+}(x,y)
\end{aligned}
\tag{A1}
$$

and for the (scalar) gluons ($D = G$) as

$$
\begin{aligned}
iG^c(x,y) &= \left\langle T\chi^{a,r}(x)\chi^{b,s}(y)\right\rangle - \langle\chi^{a,r}(x)\rangle \left\langle \chi^{b,s}(y)\right\rangle = iG^{--}(x,y)\\
iG^a(x,y) &= \left\langle \tilde{T}\chi^{a,r}(x)\chi^{b,s}(y)\right\rangle - \langle\chi^{a,r}(x)\rangle \left\langle \chi^{b,s}(y)\right\rangle = iG^{++}(x,y)\\
iG^>(x,y) &= \left\langle \chi^{a,r}(x)\chi^{b,s}(y)\right\rangle - \langle\chi^{a,r}(x)\rangle \left\langle \chi^{b,s}(y)\right\rangle = iG^{+-}(x,y)\\
iG^<(x,y) &= \left\langle \chi^{b,s}(y)\chi^{a,r}(x)\right\rangle - \langle\chi^{a,r}(x)\rangle \left\langle \chi^{b,s}(y)\right\rangle = iG^{-+}(x,y).
\end{aligned}
\tag{A2}
$$

Here $T$ and $\tilde{T}$ are the usual time and anti-time ordering operators respectively. Our convention follows that of Ref. [12]. The Wigner Transform of the Green functions is given by

$$
D(X,p) = \int d^4u\, e^{ip*u}\, D\left(X+\frac{u}{2}, X-\frac{u}{2}\right) \tag{A3}
$$

with the center of mass variable $X = x + y$ and the relative distance $u = x - y$.

In a standard fashion, the equations of motion for the Wigner transform of these Green functions, the so-called transport and constraint equations, can be derived [6]. They read

$$
-2ip\partial_X D^{-+}(X,p) = I_{\rm coll} + I^A_- + I^R_- \qquad \text{transport} \tag{A4}
$$

and

$$
\left(\frac{1}{2}\Box_X - 2p^2 + 2M^2\right) D^{-+}(X,p) = I_{\rm coll} + I^A_+ + I^R_+ \qquad \text{constraint,} \tag{A5}
$$

respectively, where $M$ is a generic parton mass, $M = m$ for the gluons and $M = 0$ for the quarks. $I_{\rm coll}$ is the collision term

$$
\begin{aligned}
I_{\rm coll} &= \Pi^{-+}(X,p)\hat{\Lambda}D^{+-}(X,p) - \Pi^{+-}(X,p)\hat{\Lambda}D^{-+}(X,p)\\
&= I^{\rm gain}_{\rm coll} - I^{\rm loss}_{\rm coll}.
\end{aligned}
\tag{A6}
$$

$I^R_\mp$ and $I^A_\mp$ are terms containing retarded and advanced components respectively,

$$I^R_{\mp} = -\Pi^{-+}(X,p)\hat{\Lambda}D^R(X,p) \pm D^R(X,p)\hat{\Lambda}\Pi^{-+}(X,p) \tag{A7}$$

and

$$I^A_{\mp} = \Pi^A(X,p)\hat{\Lambda}D^{-+}(X,p) \mp D^{-+}(X,p)\hat{\Lambda}\Pi^A(X,p). \tag{A8}$$

In Eqs.(A6) to (A8), the operator $\hat{\Lambda}$ is given by

$$\hat{\Lambda} := \exp\left\{\frac{-i}{2}\left(\overleftarrow{\partial}_X\overrightarrow{\partial}_p - \overleftarrow{\partial}_p\overrightarrow{\partial}_X\right)\right\} \tag{A9}$$

and it is set to 1 in the following calculations, which corresponds to the semi-classical approximation obtained ($\hbar = 1$).

For the calculation of the self-energies, it is useful to introduce the quasiparticle approximation, in which a *free* scalar parton of mass $M$ is assigned the Green functions

$$iD^{-+}(X,p) = \frac{\pi}{E_p}\{\delta(E_p - p^0)f_a(X,p) + \delta(E_p + p^0)\bar{f}_{\bar{a}}(X,-p)\} \tag{A10}$$

$$iD^{+-}(X,p) = \frac{\pi}{E_p}\{\delta(E_p - p^0)\bar{f}_a(X,p) + \delta(E_p + p^0)f_{\bar{a}}(X,-p)\} \tag{A11}$$

$$\begin{aligned} iD^{--}(X,p) &= \frac{i}{p^2 - M^2 + i\epsilon} + \Theta(-p^0)iD^{+-}(X,p) + \Theta(p^0)iD^{-+}(X,p) \\ &= \frac{i}{p^2 - M^2 + i\epsilon} + \frac{\pi}{E_p}\{\delta(E_p - p^0)f_a(X,p) + \delta(E_p + p^0)f_{\bar{a}}(X,-p)\} \end{aligned} \tag{A12}$$

$$\begin{aligned} iD^{++}(X,p) &= \frac{-i}{p^2 - M^2 - i\epsilon} + \Theta(-p^0)iD^{+-}(X,p) + \Theta(p^0)iD^{-+}(X,p) \\ &= \frac{-i}{p^2 - M^2 - i\epsilon} + \frac{\pi}{E_p}\{\delta(E_p - p^0)f_a(X,p) + \delta(E_p + p^0)f_{\bar{a}}(X,-p)\} \end{aligned} \tag{A13}$$

with $E_p^2 = p^2 + M^2$, and which are given in terms of the corresponding scalar quark and gluon distribution function, $f_a(X,p)$, and $\bar{f}_a = 1 + f_a$, where $a$ denotes the parton type $a = q, g$.

# REFERENCES


[1] W. Botermans and R. Malfliet, Phys. Rep. 198 (1990) 115; K.-C. Chou, Z.-B. Su, B.-L. Hao, and L. Yu, Phys. Rep. 118 (1985) 1.

[2] K. Geiger and B. Müller, Nuc. Phys. B 369 (1992) 600.

[3] K. Geiger, Phys. Rev. D 54 (1996) 949; U. Heinz, Phys. Rev. Lett. 51 (1983) 351; H.-T. Elze and U. Heinz, Phys. Rep. 183 (1989) 81.

[4] S.P. Klevansky, A. Ogura, and J. Hüfner, Ann. Phys. (N.Y.) 261 (1997) 261.

[5] S. Mrówczyński and U. Heinz, Ann. Phys. (N.Y.) 229 (1994) 1.

[6] D.S. Isert, S.P. Klevansky, hep-ph/9905289 (1999).

[7] J. Schwinger, J. Math. Phys. 2 (1961) 407; L.V. Keldysh, JETP 20 (1965) 1018.

[8] H. Umezawa, Advanced Field Theory, Micro, Marco, and Thermal Physics (American Institute of Physics, New York, 1993).

[9] T. Altherr and D. Seibert, Phys. Lett. B333 (1994) 149; T. Altherr, Phys. Lett. B341 (1995) 325.

[10] C. Greiner and S. Leupold, Eur. Phys. J. C8 (1999) 517.

[11] I. Dadić, Phys. Rev. D 59 (1999) 125012.

[12] L.D. Landau and E.M. Lifschitz, Physikalische Kinetik, vol.10 (Akademie Verlag, Berlin, 1986).

[13] J.C. Polkinghorne, J. Math. Phys. 4 (1963) 503; 4 (1963) 1393; 4 (1963) 1396.

[14] J.R. Forshaw and D.A. Ross, Quantum Chromodynamics and the Pomeron (Cambridge University Press, Cambridge, 1997) p.26.

[15] N.P. Landsman and CH.G. van Weert, Phys. Rep. 145 (1987) 141.

[16] Ch.G. van Weert, Proc. Workshop on Thermal Field Theory, Banff, 1993, ed. F.C. Khanna, R. Kobes, G. Kunstatter, and H. Umezawa (World Scientific, Singapore, 1994) p.1.

[17] H. Umezawa, H. Matsumoto, and M. Tachiki, Thermo Field Dynamics and Condensed States (North-Holland Publishing Company, Amsterdam, 1982).

[18] Y. Fujimoto and R. Grigjanis, Z. Phys. C 28 (1985) 395.

## FIGURES


FIG. 1. (a) Fock self-energy diagram and (b) Feynman diagram for the process $q\bar{q} \to g$ in lowest order.

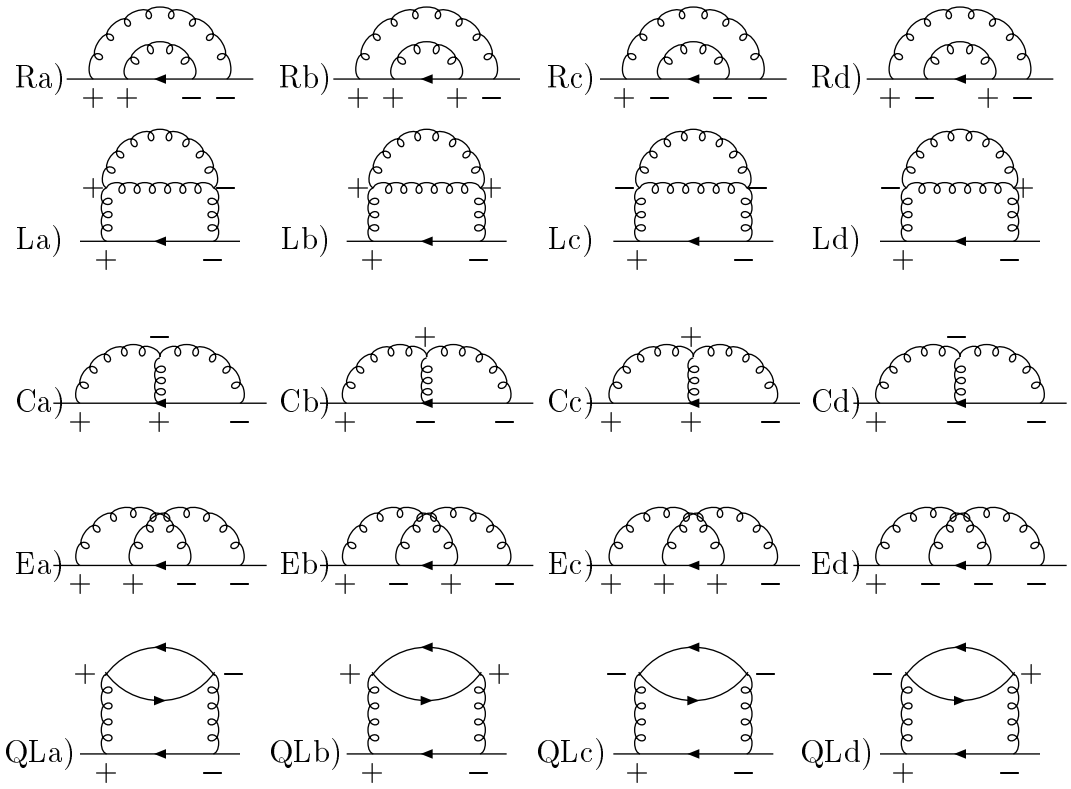


FIG. 2. Two loop self-energy diagrams contributing to $\Sigma^{(2)+-}$.

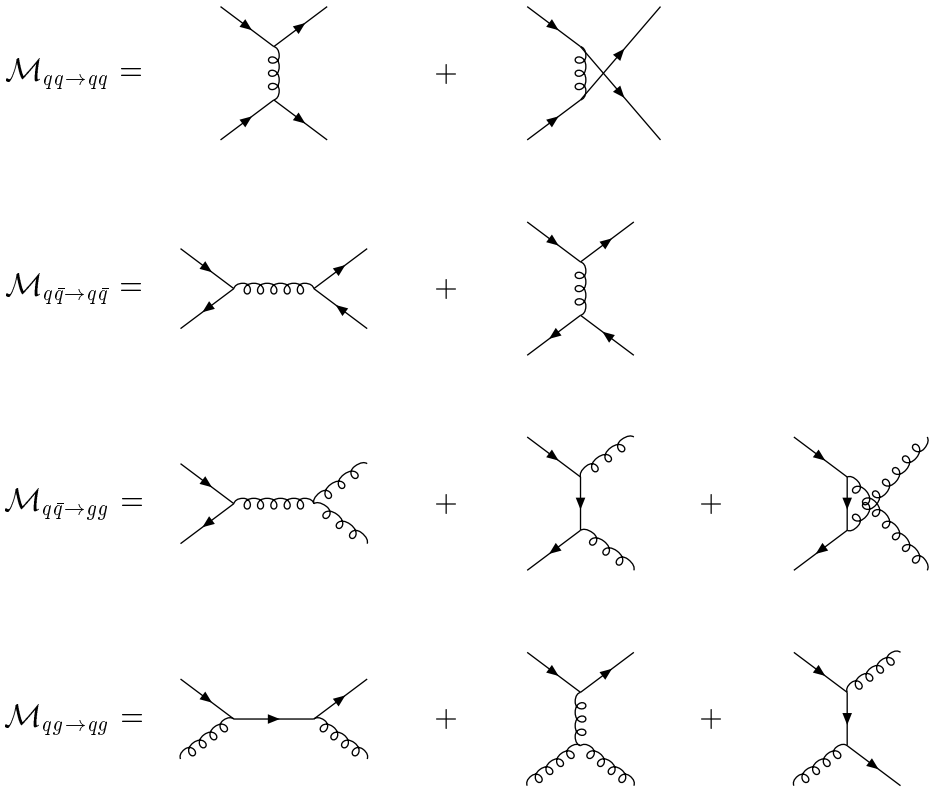


FIG. 3. Scattering amplitudes for all two → two processes.

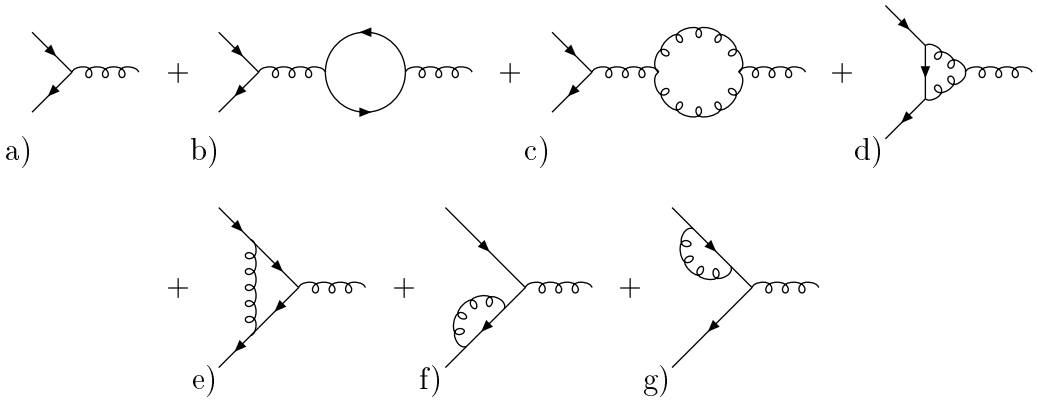


FIG. 4. Feynman diagrams for the process $q\bar{q} \to g$ up to order $g^3m^3$.

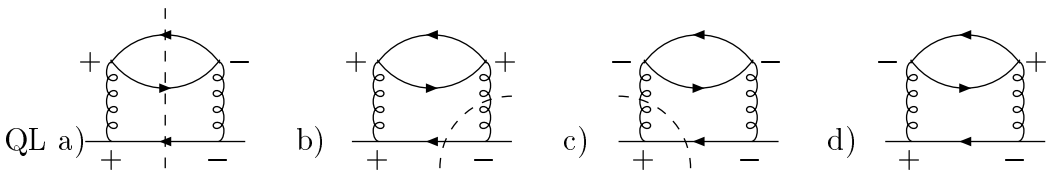


FIG. 5. Quark-loop self-energy diagrams with cut lines (dashed lines).


FIG. 6. Generic two loop self-energy diagrams for one parton type.

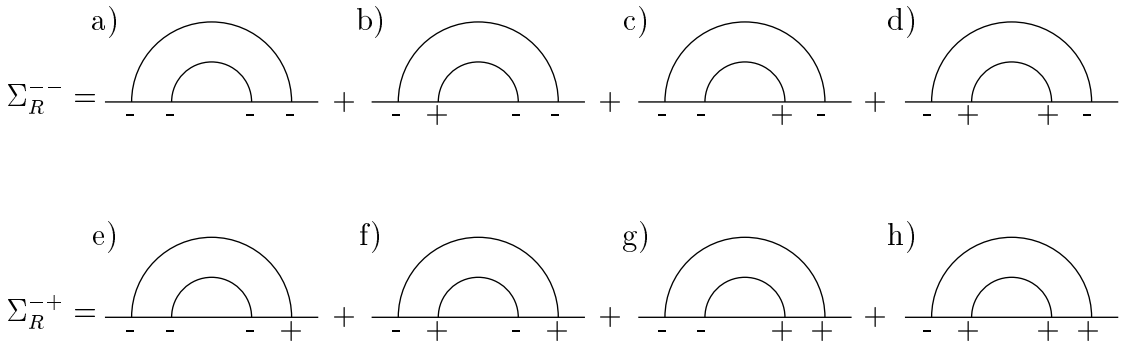


FIG. 7. Rainbow self-energy diagrams for $\Sigma_R^{--}$ and $\Sigma_R^{-+}$.